NATIONAL ADVISORY COMMITTEE FOR AERONAUTICS

TECHNICAL NOTE 3572

AMPLITUDE OF SUPERSONIC DIFFUSER FLOW PULSATIONS

By William H. Sterbentz and Joseph Davids

Lewis Flight Propulsion Laboratory
Cleveland, Ohio

Washington
October 1955

NATIONAL ADVISORY COMMITTEE FOR AERONAUTICS

TECHNICAL NOTE 3572

AMPLITUDE OF SUPERSONIC DIFFUSER FLOW PULSATIONS[1]

By William H. Sterbentz and Joseph Davids

SUMMARY

A theoretical method for evaluating the stability characteristics and the amplitude and the frequency of pulsation of ram-jet engines without heat addition is presented herein. Experimental verification of the theoretical results are included where data were available.

Theory and experiment show that the pulsation amplitude of a high mass-flow-ratio diffuser increases with decreasing mass flow. The theoretical trends for changes in amplitude, frequency, and mean pressure recovery with changes in plenum-chamber volume were experimentally confirmed.

For perforated convergent-divergent-type diffusers, a stability hysteresis loop was predicted on the pressure-recovery, mass-flow-ratio curve. At a given mean mass-flow ratio, the higher value of mean pressure recovery corresponded to oscillatory flow in the diffuser while the lower branch was stable. This hysteresis has been observed experimentally.

The theory indicates that for a ram-jet engine of given diameter, the amplitude of pulsation of a supersonic diffuser is increased by decreasing the relative size of the plenum chamber with respect to the diffuser volume down to a critical value at which oscillations cease. In the region of these critical values, the stable mass-flow range of the diffuser may be increased either by decreasing the combustion-chamber volume or by increasing the length of the diffuser.

INTRODUCTION

Supersonic diffusers are usually selected so that at design mass flows pulsation-free operation will be obtained. However, there are conditions of operation, such as acceleration of maneuvering, which may require reduced mass flows in the unstable region. It is therefore important that both the conditions under which flow instability will be encountered and the resulting pulsation amplitudes and frequency be known.

[1]Supersedes NACA RM E52I24, "Amplitude of Supersonic Diffuser Flow Pulsations" by William H. Sterbentz and Joseph Davids, 1952.

Certain resonance criterions which reasonably predicted both the conditions for the occurrence of diffuser flow pulsations and the frequency of pulsation were evaluated assuming that a ram-jet engine acts, in effect, as a Helmholtz resonator (ref. 1). It was found that a diffuser would resonate if the subcritical diffuser characteristic had a positive slope of sufficient magnitude. At conditions where the slope of this curve was less than the critical value, the ram-jet engine would not resonate. A similar criterion for the occurrence of diffuser pulsation was suggested from analyses presented in reference 2.

The occurrence of flow pulsation in external-compression diffusers is related in reference 3 to the velocity discontinuity or vortex sheet downstream of the intersection of two shock waves. Flow pulsations start when this vortex sheet just enters or leaves the diffuser cowling. The entrance of the vortex sheet into the diffuser cowling marks a change in the slope of the diffuser characteristic which arises from the entrance of increasing percentages of low-energy mass flows. The amount of change in diffuser characteristic required to induce flow pulsations in any ram-jet engine may be readily determined from the theoretical criterions of reference 1.

Although certain theoretical criterions as to the nature of diffuser pulsation have been evaluated, no theoretical evaluation of the variables affecting amplitude has been developed. This report, prepared at the NACA Lewis laboratory, presents a theoretical evaluation of the variables which govern pulsation amplitude for the cold-flow engine. The theoretical method employed is a refinement of the diffuser-pulsation theory presented in reference 1. The method of reference 1 assumed small amplitudes of flow disturbances in order that quantities such as mass flow and the slope of the diffuser characteristic could be considered constant. When large finite amplitudes are allowed, these quantities must be recomputed in a point-to-point calculation throughout a cycle of oscillation. Several numerical computations which illustrate the nonlinear solutions for pulsation amplitudes and frequencies as a function of diffuser mass-flow ratio and geometry are included herein. Experimental data are presented for comparison with the theoretical trends where possible.

SYMBOLS

The following symbols and definitions were used in this report:

A	area, sq ft
a	velocity of sound, ft/sec
f	frequency, cycles/sec

M	Mach number
m	mass flow, slugs/sec
m_0	diffuser maximum mass flow, slugs/sec
Δm	mass-flow perturbation, slugs/sec
P	total pressure, lb/sq ft abs
ΔP	pressure perturbation, lb/sq ft
ΔP_I	pressure perturbation arising from the inertia properties of the perturbed flow, lb/sq ft
ΔP_{II}	pressure perturbation arising from changes in diffuser-shock position, lb/sq ft
t	time, sec
u	velocity, ft/sec
Δu	velocity perturbation, ft/sec
V	effective storage volume of ram jet ($V_T - V_A$), cu ft
V_A	effective air column volume, cu ft
V_T	total volume of ram jet, cu ft
W_A	mass of virtual oscillating air column, slugs
W_c	mass of gas occupying effective storage volume of ram jet, slugs
γ	ratio of specific heats
ρ	density, slugs/cu ft

Subscripts:

m	mean
0	equivalent free-stream condition
1	diffuser inlet
2	diffuser outlet
4	exhaust-nozzle outlet

THEORETICAL ANALYSIS

The basic concept employed in the analysis of the amplitude of pulsation assumes that the resonant properties of a ram-jet engine are controlled by the balance between the mass-flow-delivery characteristics of the diffuser, the storage capacity of the combustion or plenum chamber, and the discharge characteristics of the exhaust nozzle. For the engine under steady-flow conditions, the mass flow delivered to the combustion chamber is equal to the mass flow discharged from the chamber. The presence of any transient disturbance induces an unbalance in the diffuser delivery and exhaust-nozzle discharge rates leading to a periodic storage and evacuation of air mass in the combustion chamber and concomitant cyclic pressure oscillations.

A linear differential equation of motion is developed, on the basis of the Helmholtz resonator concept (ref. 1), through a systematic calculation of the terms involved in the conservation-of-mass equation as functions of the velocity perturbation of the diffuser air column and mean-flow parameters of the engine. For conditions of unstable operation, this linear vibratory system predicts a continuous increase of pulsation to infinite amplitude. In actual systems, of course, a positive damping force becomes important at sufficiently large amplitudes, thus limiting the oscillation. Such a positive damping force arises from the nonlinear characteristics of the pressure changes incurred from shock oscillations during unsteady operation of the diffuser.

From the conservation-of-mass equation

$$\Delta m_2 = \Delta m_4 + \frac{d\Delta W_c}{dt} \tag{1}$$

the differential equation of motion developed in reference 1 is as follows:

$$\frac{W_c W_A}{m_x \gamma P_2 A_1} \frac{d^2}{dt^2} \Delta u - \frac{W_c}{\gamma P_2 a_2 M_2} \left[\frac{dP_2}{dm_2} - \frac{\gamma - 1}{2} \frac{W_A}{W_c} \left(\frac{m}{m_x} \right) \frac{a_2}{A_1} M_2 \right] \frac{d}{dt} \Delta u +$$

$$\frac{1}{a_2 M_2} \left[1 - \frac{\gamma + 1}{2\gamma} \frac{m}{P_2} \frac{dP_2}{dm_2} \right] \Delta u = 0 \tag{2}$$

If second-order effects of terms involving M_2 are neglected, the mass flow m_x may be stated as

$$m_x = \frac{\gamma P_2 A_1 M_2}{a_2}$$

Multiplying by this expression for m_x and nondimensionalizing dP_2/dm_2 transforms equation (2) to

$$\frac{W_c W_A}{\gamma P_2 A_1} \frac{d^2}{dt^2} \Delta u - \left[\frac{W_c A_1}{a_2^2} \left(\frac{P_0}{m_0} \right) \frac{d\left(\frac{P_2}{P_0} \right)}{d\left(\frac{m_2}{m_0} \right)} - \frac{\gamma - 1}{2\gamma} \frac{m W_A}{A_1 P_2} \right] \frac{d}{dt} \Delta u +$$

$$\frac{\gamma P_2 A_1}{a_2^2} \left[1 - \frac{\gamma + 1}{2\gamma} \left(\frac{m}{m_0} \right) \left(\frac{P_0}{P_2} \right) \frac{d\left(\frac{P_2}{P_0} \right)}{d\left(\frac{m_2}{m_0} \right)} \right] \Delta u = 0 \qquad (2a)$$

Small oscillations were assumed in reference 1 so that the coefficients of the differential equation could be treated as constant values. When large finite amplitudes are allowed, the variation in quantities such as $\frac{d(P_2/P_0)}{d(m_2/m_0)}$, P_2, a_2, and m throughout the cycle must be included. However, equation (2a) can still be applied in a point-to-point calculation assuming constant coefficients provided that the increments in the cycle are small enough. (The coefficients are, of course, the instantaneous values and thus are recomputed for each point.)

To obtain results for specific diffusers requires a choice of a "frozen-state" pressure-recovery mass-flow-ratio curve. The "frozen-state" pressure recovery is defined as that recovery which would be obtained across the diffuser if steady-flow conditions could be imposed. This curve may generally be estimated from the specific diffuser geometry, the shock configuration, and the diffuser friction losses.

For a high-mass-flow-ratio single-cone diffuser, peak frozen-state pressure recovery will occur at critical mass flow. Pressure losses at this condition for such a diffuser will be incurred from a shock configuration consisting of one oblique shock followed by a normal shock plus the estimated subsonic diffuser loss. For lower mass flows, the frozen-state pressure recovery decreases because decrements in mass flow from the critical condition are marked by the entrance of increasing percentages of low-energy mass flows into the inlet as the vortex sheet

moves progressively closer to the diffuser centerbody. At zero mass flow, the diffuser pressure recovery will be approximately the recovery computed across a normal shock at free-stream Mach number. For the purposes of this report, it is considered sufficiently accurate to define the frozen-state diffuser pressure recovery as varying linearly with mass-flow ratio from critical to zero mass flow for the high-mass-flow-ratio single-cone diffuser (fig. 1(a)).

For low-mass-flow-ratio single-cone diffusers, peak pressure recovery will occur at some value of subcritical mass-flow ratio. The range of mass-flow ratios from critical to peak pressure recovery is characterized by approximately constant total-pressure flow. At further reduced mass flows, the frozen-state pressure recovery continuously decreases as the vortex sheet enters the inlet and progressively advances toward the diffuser cone. By the method presented in reference 4, the entrance of the vortex sheet into the inlet and the decrement in pressure recovery with mass-flow ratio is easily computed for any single-cone diffuser. The low-mass-flow curve can again be approximated by straight line segments as in figure 1(b).

Certain cone-type diffusers encounter flow separation from the cone surface at reduced mass flows. At present it is not possible to predict the mass-flow ratio at which this separation will occur or the decrement in pressure recovery it will induce. The method of reference 5, however, does predict whether or not a cone-type diffuser will encounter flow separation.

Another type of frozen-state diffuser pressure-recovery mass-flow-ratio curve easily established is that curve commonly obtained with open-nosed, convergent-divergent, perforated diffusers. For this inlet, peak pressure recovery will occur at approximately critical mass flow. The theoretical frozen-state pressure recovery varies linearly along a line with decrements in mass-flow ratio from critical such as to maintain constant Mach number at the diffuser throat until normal-shock pressure recovery at free-stream conditions is reached. This portion of the curve (fig. 1(c)) represents the shock in the convergent section of the diffuser. The pressure recovery then remains constant at normal-shock values with further decrements in mass-flow ratio and this portion of the curve represents the normal shock ahead of the inlet.

After the frozen-state diffuser characteristics are determined, the shape of the composite curve of motion and the mean diffuser characteristics under oscillating conditions are obtained in the following manner: In equation (2a) the following substitutions may be made:

$$\Delta\dot{u} = \frac{d}{dt}\Delta u$$

$$\frac{d\Delta\dot{u}}{d\Delta u}\Delta\dot{u} = \frac{d^2}{dt^2}\Delta u$$

Also, the following quantities are assumed to be equivalent:

$$W_c = \rho_2 V$$

$$W_A = \rho_2 V_A$$

$$a_2^2 = \frac{\gamma P_2}{\rho_2}$$

Thus equation (2a) becomes, after simplification,

$$\frac{d\Delta\dot{u}}{d\Delta u} = \left(\frac{P_0}{m_0}\right)\left(\frac{A_1^2}{V_A}\right)\frac{d\left(\frac{P_2}{P_0}\right)}{d\left(\frac{m_2}{m_0}\right)} - \frac{\gamma-1}{2\gamma}\left(\frac{ma_2^2}{P_2}\right)\frac{1}{V} - a_2^2\left(\frac{A_1^2}{V_A V}\right)\left[1 - \frac{\gamma+1}{2\gamma}\left(\frac{m}{m_0}\right)\left(\frac{P_0}{P_2}\right)\frac{d\left(\frac{P_2}{P_0}\right)}{d\left(\frac{m_2}{m_0}\right)}\right]\frac{\Delta u}{\Delta\dot{u}} \tag{3}$$

Equation (3) describes a system of curves which relates the variation of air-column perturbation velocity Δu with the air-column perturbation acceleration $\Delta\dot{u}$. This relation permits the drawing of tangential directions in the coordinate system for the coordinates Δu and $\Delta\dot{u}$. For example, for $\Delta\dot{u} = 0$, the slope $d\Delta\dot{u}/d\Delta u$ is infinite in the subcritical flow region and for $\Delta u = 0$, the slope $d\Delta\dot{u}/d\Delta u$ is equal to the quantity

$$\left(\frac{P_0}{m_0}\right)\left(\frac{A_1^2}{V_A}\right)\frac{d\left(\frac{P_2}{P_0}\right)}{d\left(\frac{m_2}{m_0}\right)} - \frac{\gamma-1}{2\gamma}\left(\frac{ma_2^2}{P_2}\right)\frac{1}{V}$$

The proper values of pressure, temperature, and mass flow occurring in the coefficients of equation (3) are determined by successive approximation at each point. The mass-flow change given by equation (7) of reference 1 stated in terms of Δu and $\Delta\dot{u}$ is

$$\frac{\Delta m}{m_0} = \frac{1}{\gamma P_2}\left(\frac{m}{m_0}\right)(\Delta P_I + \Delta P_{II}) + \frac{\gamma P_2 A_1}{m_0 a_2^2}\Delta u \tag{4}$$

where the pressure changes are

$$\Delta P_I = - \frac{\gamma P_2 V_A}{a_2^2 A_1} \Delta \dot{u}$$

or stating P_2 in terms of $P_{2,m}$, ΔP_I, and ΔP_{II}

$$\Delta P_I = \frac{- \left(\frac{\gamma V_A}{a_2^2 A_1} \right) (P_{2,m} + \Delta P_{II}) \Delta \dot{u}}{1 + \frac{\gamma V_A}{a_2^2 A_1} \Delta \dot{u}} \tag{5}$$

and ΔP_{II} is equal to the change in frozen-state pressure recovery from the mean. The change in a_2^2 arising from adiabatic temperature changes is

$$a_2^2 = a_{2,m}^2 \left(\frac{P_2}{P_{2,m}} \right)^{\left(\frac{\gamma - 1}{\gamma} \right)} \tag{6}$$

where $a_{2,m}$ and $P_{2,m}$ are the respective mean values of the diffuser-outlet acoustic velocity and pressure.

An example of the use of equations (4), (5), and (6) follows. It is desired to establish the critical mass-flow curve on a $\Delta \dot{u}$ against Δu chart for some fixed mean value of mass-flow ratio. The origin on this chart, of course, represents the mean mass-flow conditions of the problem. The quantities immediately known are $\Delta m/m_0$, $P_{2,m}$, ΔP_{II}, $a_{2,m}$, the geometrical constants, and the variable $\Delta \dot{u}$. Quantities to be determined are ΔP_I, P_2, a_2, and the appropriate values of the variable Δu.

By successive approximations using equations (5) and (6), the values of ΔP_I, P_2, and a_2 are easily established for any fixed value of $\Delta \dot{u}$. (It should be noted that pressure P_2 is the sum of the mean pressure $P_{2,m}$ and the pressure changes ΔP_I and ΔP_{II}.) These quantities, when substituted in equation (4), permit the evaluation of Δu and the establishment of one point on the $\Delta \dot{u}$ against Δu chart representing critical flow conditions. When this calculation is repeated for other values of $\Delta \dot{u}$, the complete critical mass-flow curve is established. Other subcritical mass-flow-ratio curves are established in this same manner.

The equation defining the supercritical mass-flow curve is

$$\gamma^2\left(\frac{m_0}{m}\right)\left(\frac{P_2}{a_2}\right)^2 A_1 V\Delta\dot{u} + \frac{\gamma(\gamma+1)}{2} P_2 m_0 A_1 \Delta u - \frac{\gamma-1}{2} a_2^2 m_0^2\left(\frac{\Delta m_2}{m_0}\right) = 0 \qquad (7)$$

This equation is obtained from a substitution of equations (7), (11), and (12) into equation (10) of reference 1. For any given value of Δu, the value of the instantaneous pressure P_2 and the acoustic velocity a_2 may readily be determined by successive approximations from equation (4). Thus, if the values of P_2 and a_2 for a given value of Δu are known, the proper value of $\Delta\dot{u}$ may be computed from equation (7). The repetition of this calculation for other values of Δu establishes the complete supercritical mass-flow-ratio curve.

An illustrative solution of equation (3) is plotted in figure 2 which presents a coordinate system of $\Delta\dot{u}$ as a function of Δu. The graph is divided into the subcritical and supercritical flow regions by the method just described. Starting at $\Delta u = -600$ feet per second and $\Delta\dot{u} = 0$, the curve goes around in a clockwise direction until supercritical flow conditions in the diffuser are established, and thereafter describes a closed figure continuously. Also, starting from rest ($\Delta\dot{u} = 0$ and $\Delta u = 0$), the same closed curve is reached after a number of increasing clockwise spiral turns.

The variation of Δu as a function of time t is obtained from a second graphical integration and the results of the example are shown in figure 3. The abscissa of a point on figure 2 is represented on the ordinate of figure 3 and the ordinate of a point on figure 2 is the slope of the curve on figure 3. Starting from the origin, the amplitude of Δu gradually increases with time until the value of the final or natural amplitude is reached. For the case where the initial disturbance is larger than the final value of amplitude, the pulsation diminishes with time to the final amplitude. By use of equations (4), (5), and (6) and the graphical variation of Δu and $\Delta\dot{u}$ with time, the variation of ram-jet plenum-chamber pressure may be readily obtained.

Some of the effects of changes in engine geometry, flow conditions, and diffuser characteristics will be evaluated and compared with available experimental data in the following discussion. All theoretical amplitude and frequency curves presented were evaluated by the foregoing method.

RESULTS AND DISCUSSION

High-Mass-Flow-Ratio Diffuser

Comparisons of the theoretical and experimental pulsation amplitude and frequency for a high-mass-flow-ratio diffuser with two plenum-chamber volumes at a free-stream Mach number of 2.0 is presented in figure 4. Schematic drawings of the ram-jet engine and diffuser are shown in figure 5. One experimental frequency data point was used to establish the proper value of V_A required in equation (3) and this point is tailed in figure 4(b). The remainder of the frequency curves and the resulting pulsation amplitudes for both plenum-chamber volumes were then computed using this value for the volume V_A. The value of the ratio of the virtual oscillating air column to the total ram-jet engine volume V_A/V_T for the small plenum-chamber engine was 0.740 and for the large plenum-chamber engine, 0.323.

The theoretical variation and magnitude of pulsation amplitude with both volumes is in good agreement with experiment over the range of mass flows investigated. The amplitude increased steadily with decreases in mass-flow ratio. In both cases, experimental frequency decreased gradually with increasing mass-flow ratio compared with the nearly constant value predicted by theory. The experimental amplitude and frequency decreased as the plenum-chamber volume was increased as predicted by the theory.

From the integration of the pressure-time diagram of a flow pulsation (such as shown on fig. 6), the average increment or decrement in the frozen-state value of diffuser pressure recovery which results from the pulsation can be computed. The resulting curves are included in figure 4(c). Flow pulsation caused a decrease in pressure recovery below that value assumed for the frozen-state pressure recovery to a mass-flow ratio of about 0.61 for the small volume engine and to about 0.48 for the large volume engine, after which an increase was computed. A theoretical effect of an increase in diffuser pressure recovery caused by a decrease in plenum-chamber volume was also noted experimentally. However, the experimental rise in pressure recovery with mass-flow ratio in the range $0.46 \leq m_2/m_0 \leq 0.62$ was not predicted by the theory. The discrepancies may be partly due to the crudity of the assumed frozen-state pressure-recovery mass-flow curve.

No flow pulsations were found by computation to be sustained for supercritical flow conditions and all transient disturbances were found to be damped out.

The theoretical pressure-time wave form only approximately predicts the experimental pressure-time fluctuations as can be noted from figure 6. Some variations from the experimental values are to be expected

because of the simplifying assumptions included in the analysis. A closer agreement of the theoretical and experimental wave forms at equilibrium by a different analysis is presented in reference 6.

Open-Nosed, Convergent-Divergent, Perforated Diffuser

In the foregoing analysis of the properties of a high-mass-flow-ratio diffuser, small point-to-point increments in mass flow, pressure, and temperature were used to recompute the point-to-point values of the coefficients of equation (3) in obtaining the theoretical solutions. To conserve time and labor in the following solutions, only a few large increments of mass flow, pressure, and temperature were used. Thus, the general trends will still be the same although, if smaller increments were employed in the calculation, absolute values of the results would be somewhat changed.

A theoretical solution of the pulsation characteristics of an arbitrary, hypothetical, open-nosed, convergent-divergent, perforated diffuser was obtained (see fig. 7). Two modes of operation were found to be theoretically possible. In the first mode, if the diffuser were started in the zero mass-flow condition with no flow oscillations, pulsation-free flow with approximately free-stream normal-shock recovery would persist over the mass-flow-ratio range to 0.50. At a mass-flow ratio of 0.50, however, flow pulsations will set in and the diffuser pressure recovery will increase several percentage points. Flow pulsations, once started, were found theoretically to persist over the entire subcritical mass-flow range. This stability hysteresis is defined, by theory, to arise from a critical pulsation amplitude such that flow perturbations less than this critical value are damped out, whereas perturbations greater than this critical value are amplified as an oscillatory disturbance to a new natural amplitude. For this particular hypothetical diffuser, the critical amplitude is approximately the flow disturbance necessary to induce instantaneous values of the mass-flow ratio greater than 0.50. The variation of values of the critical and the natural amplitude with mass-flow ratio are shown on figure 7.

The existence of a stability hysteresis and the rise in diffuser pressure recovery with the onset of flow pulsation are confirmed by experiments reported in reference 7. Reference 7 presents the performance of a series of perforated, convergent-divergent diffusers having numerous contraction ratios and perforation distributions. Typical of the results of this investigation are the data plotted in figure 8 for the 1.63-e-contraction-ratio diffuser obtained from figure 17(u) of reference 7. The lower branch of the hysteresis curve was generally obtained when the tunnel flow was first initiated. When the mass-flow

ratio was increased into the unstable region (from about 0.48 to 0.82), the mean-pressure recovery jumped to its oscillatory value. The diffuser then continued to operate on the upper or oscillatory curve even to nearly zero mass flow through this diffuser.

Some Additional Theoretical Trends

The effects on amplitude and frequency of varying plenum-chamber volume V or diffuser-air-column volume V_A are shown in figures 9 and 10. In figure 9, the plenum-chamber volume is varied while the diffuser volume is held constant. As the plenum-chamber volume is progressively decreased, the pulsation amplitude and frequency gradually increase until a critical value is reached at which pulsations cease. In this region, the stable mass-flow range of a supersonic diffuser may be improved by further reductions in plenum-chamber volume.

In figure 10, the air-column or diffuser volume is varied while the plenum-chamber volume is held constant. In this case, as the diffuser volume is increased, the pulsation amplitude increases and frequency decreases. Again, a critical ratio of plenum-chamber volume to diffuser volume exists such that further increases in diffuser volume progressively increase the stable mass-flow-ratio range of the diffuser.

Thus, from figures 9 and 10, it can be noted that for any ram-jet engine of given diameter, the amplitude of pulsation of a supersonic diffuser may be decreased by increasing the relative size of the plenum-chamber volume with respect to the air-column or diffuser volume. Also, the frequency of pulsation for any ram-jet engine of given diameter will be decreased as either diffuser volume or plenum-chamber volume or both are increased.

SUMMARY OF RESULTS

The following summary presents the theoretical and experimental results of the effects of engine geometry and diffuser-flow conditions on supersonic diffuser pulsation amplitude and frequency.

1. Theory and experiment show that pulsation amplitude of a high-mass-flow ratio diffuser increases with decreasing mass-flow ratio. The theoretical trends for changes in amplitude, frequency, and mean pressure recovery with changes in combustion-chamber volume were experimentally confirmed.

2. For perforated convergent-divergent-type diffusers a stability hysteresis loop was predicted on the pressure-recovery mass-flow-ratio curve. At a given mean mass-flow ratio, the higher value of mean-pressure

recovery corresponded to oscillatory flow in the diffuser while the lower branch was stable. This hysteresis has been observed experimentally.

3. The theory indicates that for a ram-jet engine of given diameter, the amplitude of pulsation of a supersonic diffuser is increased by decreasing the relative size of the plenum chamber with respect to the diffuser volume to a critical value at which oscillations cease. In the region of these critical values, the stable mass-flow range of the diffuser may be increased either by decreasing the combustion-chamber volume or by increasing the length of the diffuser.

Lewis Flight Propulsion Laboratory
National Advisory Committee for Aeronautics
Cleveland, Ohio, August 20, 1952

REFERENCES

1. Sterbentz, William H., and Evvard, John C.: Criterions for Prediction and Control of Ram-Jet Flow Pulsations. NACA RM E51C27, 1951.

2. Pearce, R. B.: Causes and Control of Powerplant Surge. Aviation Week, vol. 52, no. 3, Jan. 16, 1950, pp. 21-25.

3. Ferri, Antonio, and Nucci, Louis M.: The Origin of Aerodynamic Instability of Supersonic Inlets at Subcritical Conditions. NACA RM L50K30, 1951.

4. Moeckel, W. E.: Approximate Method for Predicting Form and Location of Detached Shock Waves Ahead of Plane or Axially Symmetrical Bodies. NACA TN 1921, 1949.

5. Reshotko, Eli, and Tucker, Maurice: Effect of a Discontinuity on Turbulent Boundary-Layer-Thickness Parameters with Application to Shock-Induced Separation. NACA TN 3454, 1955.

6. Trimpi, Robert L.: An Analysis of Buzzing in Supersonic Ram Jets by a Modified One-Dimensional Non-Stationary Wave Theory. NACA RM L52A18, 1952.

7. Hunczak, Henry R., and Kremzier, Emil J.: Characteristics of Perforated Diffusers at Free-Stream Mach Number 1.90. NACA RM E50B02, 1950.

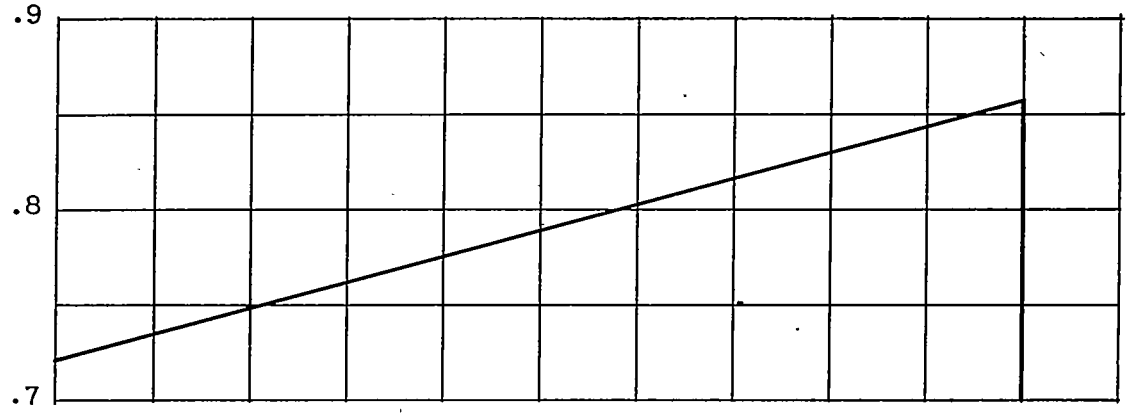

(a) High-mass-flow-ratio diffuser.

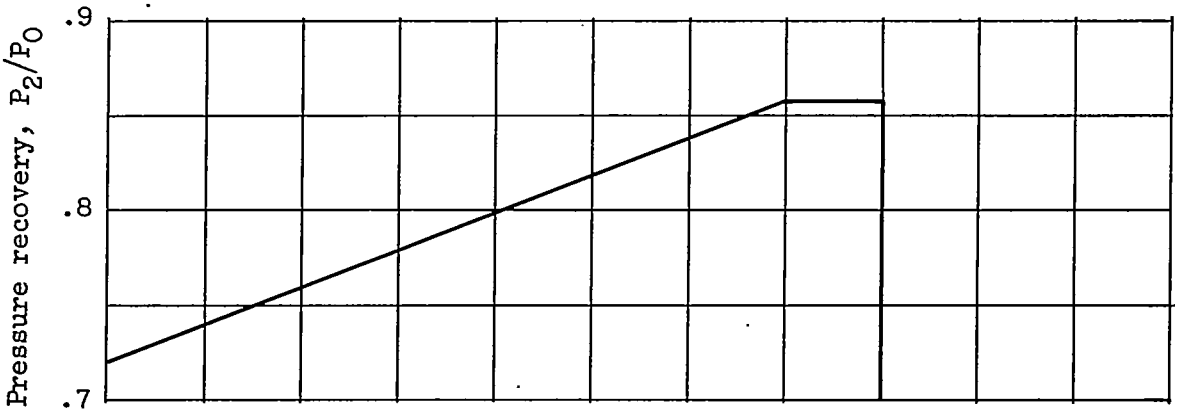

(b) Low-mass-flow-ratio diffuser.

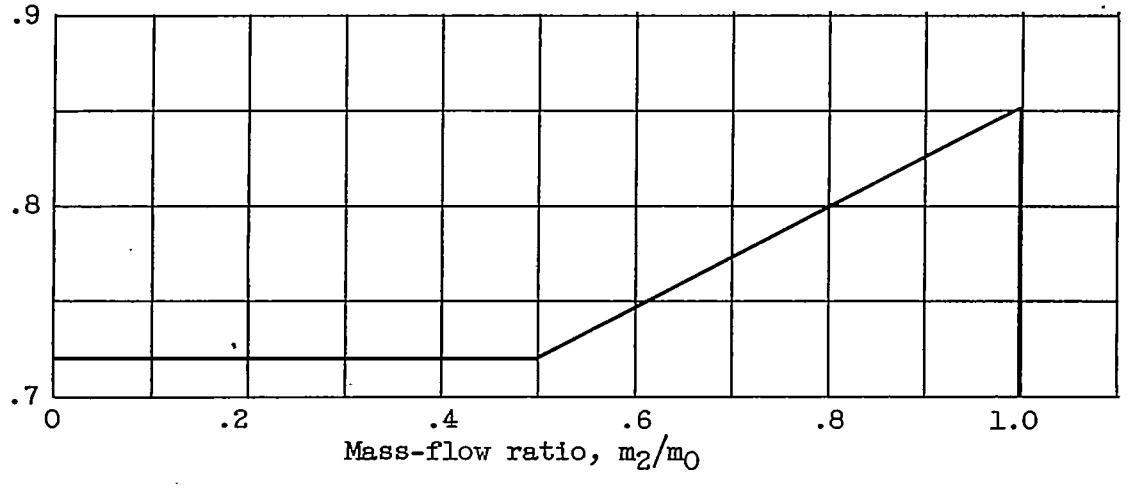

(c) Open-nosed, convergent-divergent, perforated diffuser.

Figure 1. - Typical variation of frozen-state pressure recovery with mass-flow ratio for three diffusers.

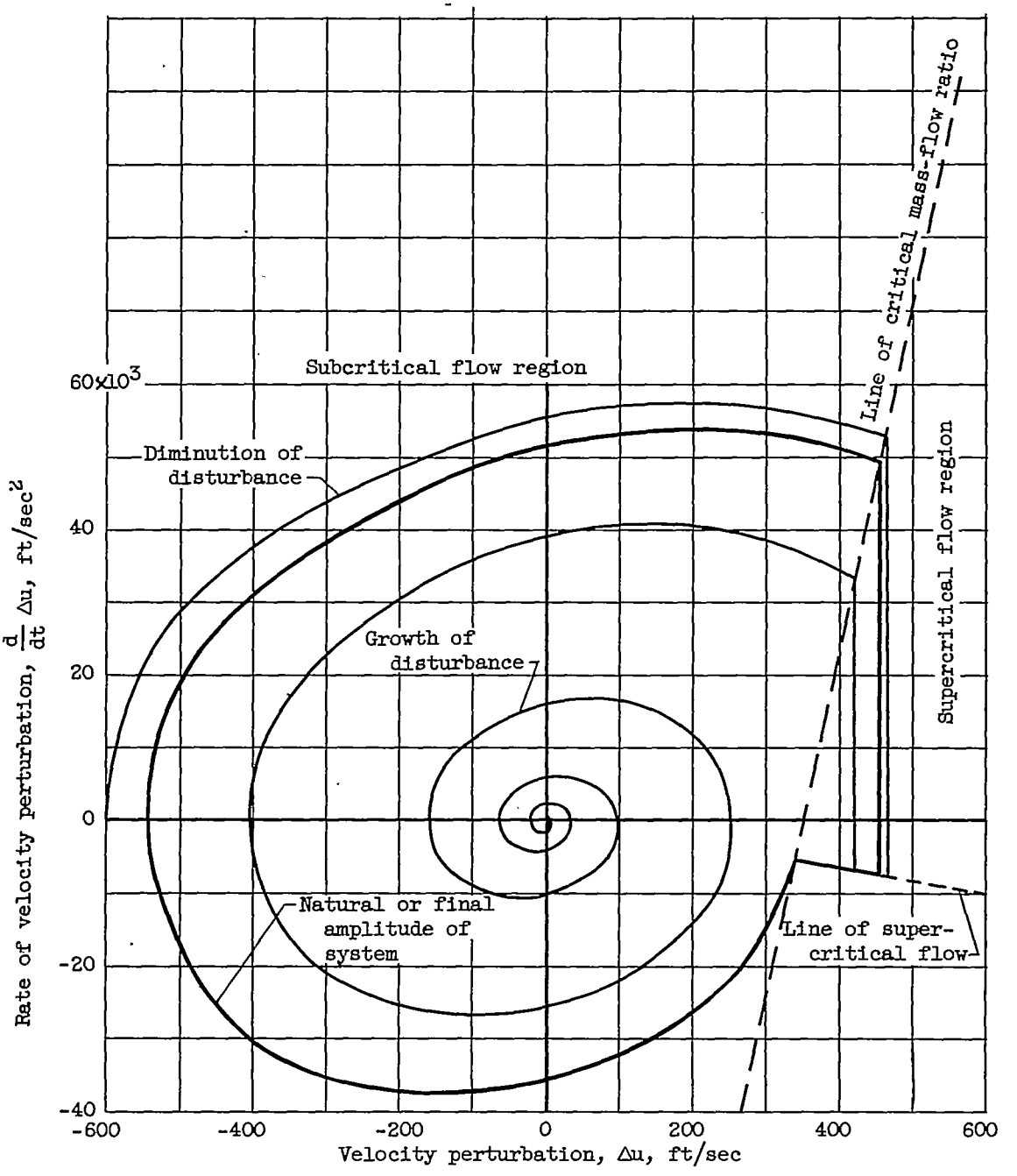

Figure 2. - Illustrative example of theoretical growth of minute transient disturbance and diminution of large transient disturbance to natural amplitude of arbitrary ram jet at fixed mean mass-flow ratio and free-stream Mach number. First integration.

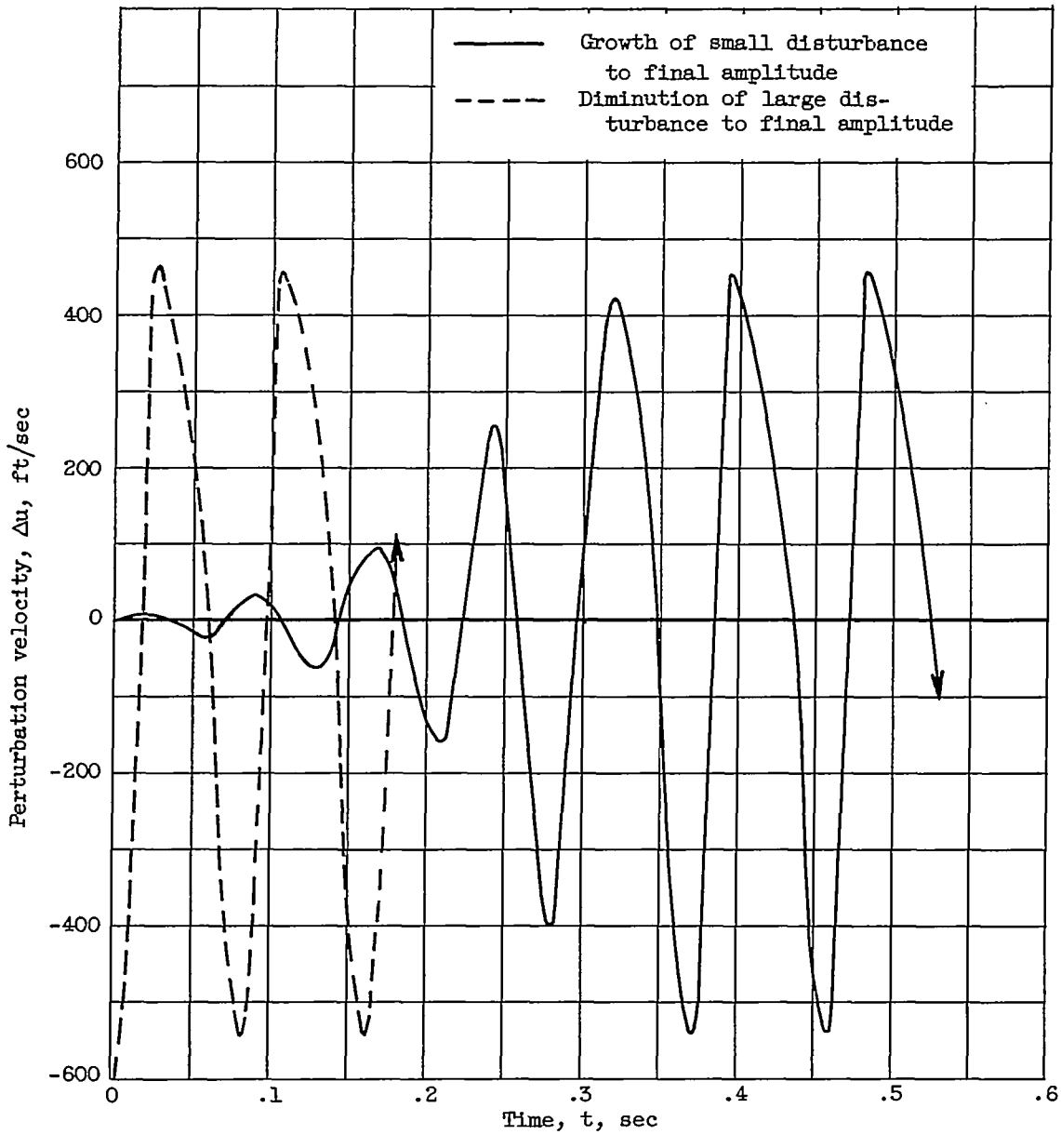

Figure 3. - Second integration of growth and diminution of transient disturbances presented in figure 2.

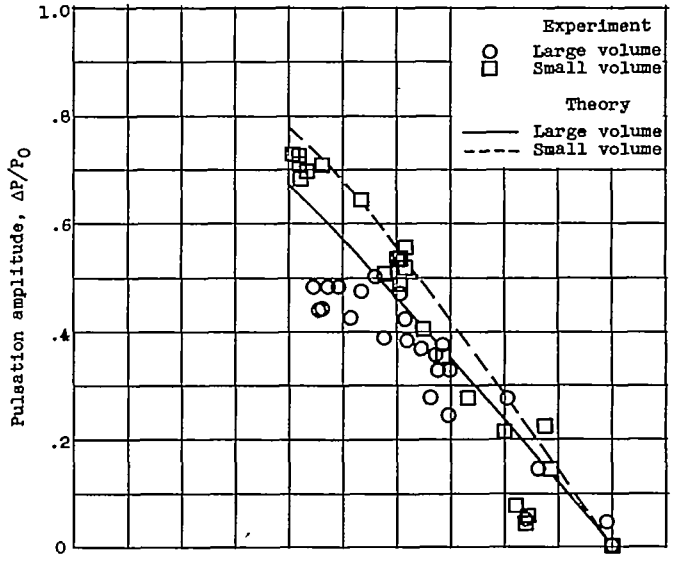

(a) Amplitude.

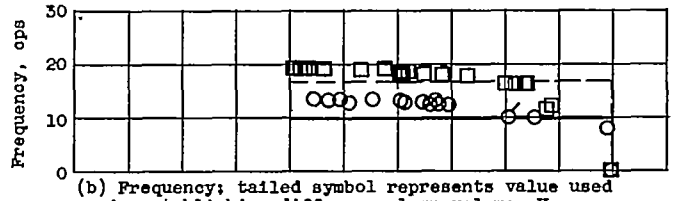

(b) Frequency; tailed symbol represents value used in establishing diffuser-column volume, V_A.

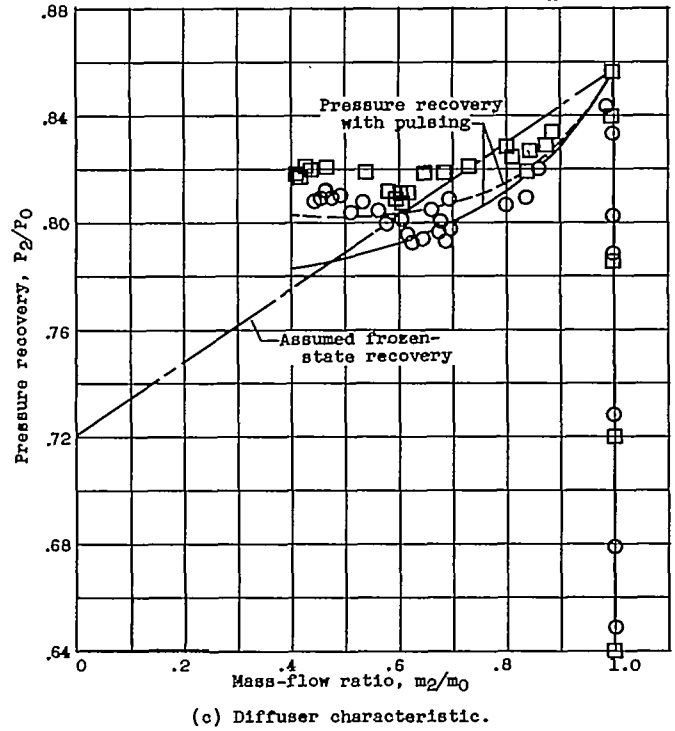

(c) Diffuser characteristic.

Figure 4. - Comparison of experimental and theoretical effect of plenum-chamber volume and mass-flow ratio on pulsation amplitude, frequency, and diffuser pressure recovery at free-stream Mach number of 2.00.

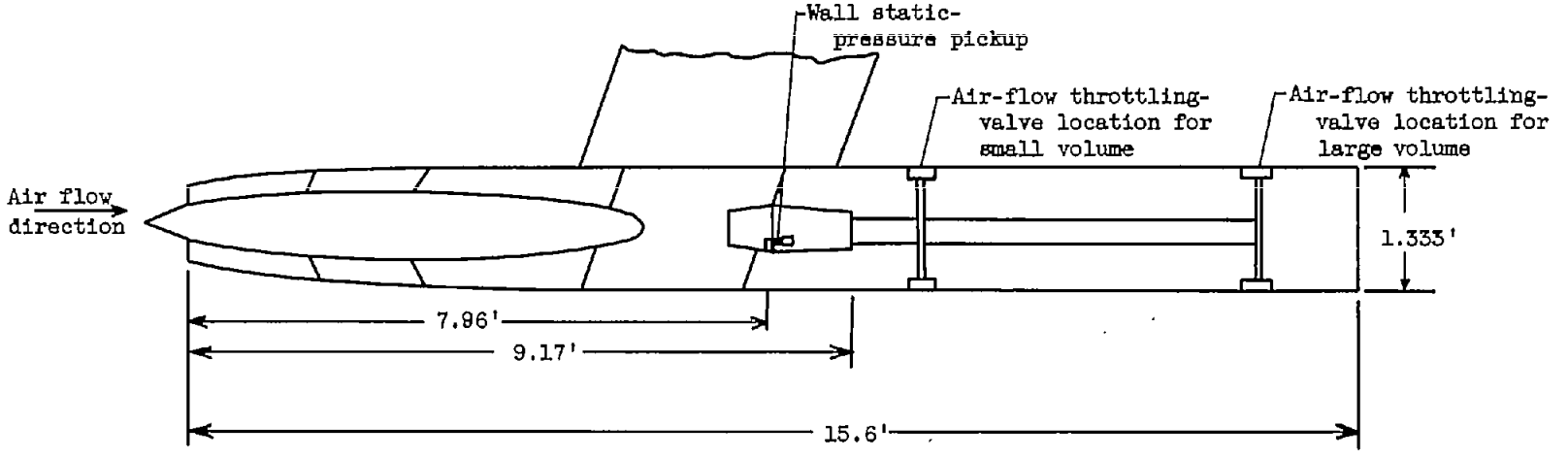

(a) Ram-jet configuration.

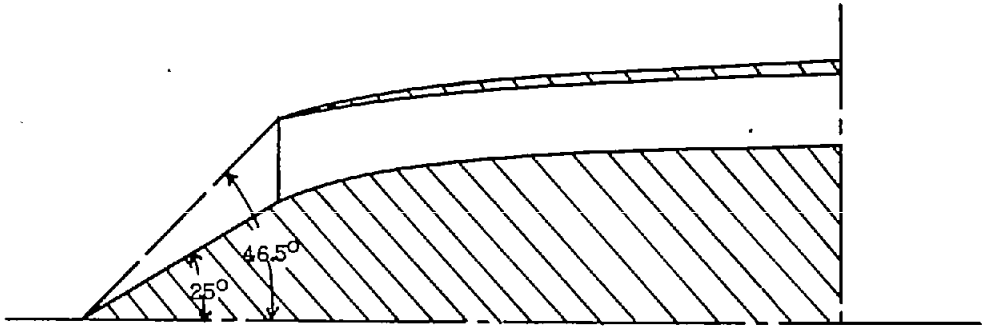

(b) High-mass-flow-ratio diffuser investigated.

Figure 5. - Schematic drawing of 16-inch ram-jet engine. Total volume (large volume engine), 12.4 cubic feet; total volume (small volume engine), 5.4 cubic feet; diffuser-throat area, 0.400 square feet.

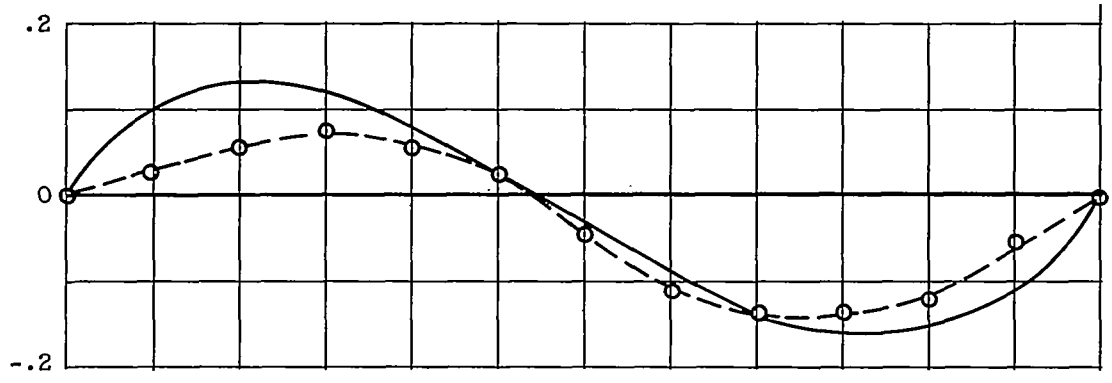

(a) Mass-flow ratio, 0.80.

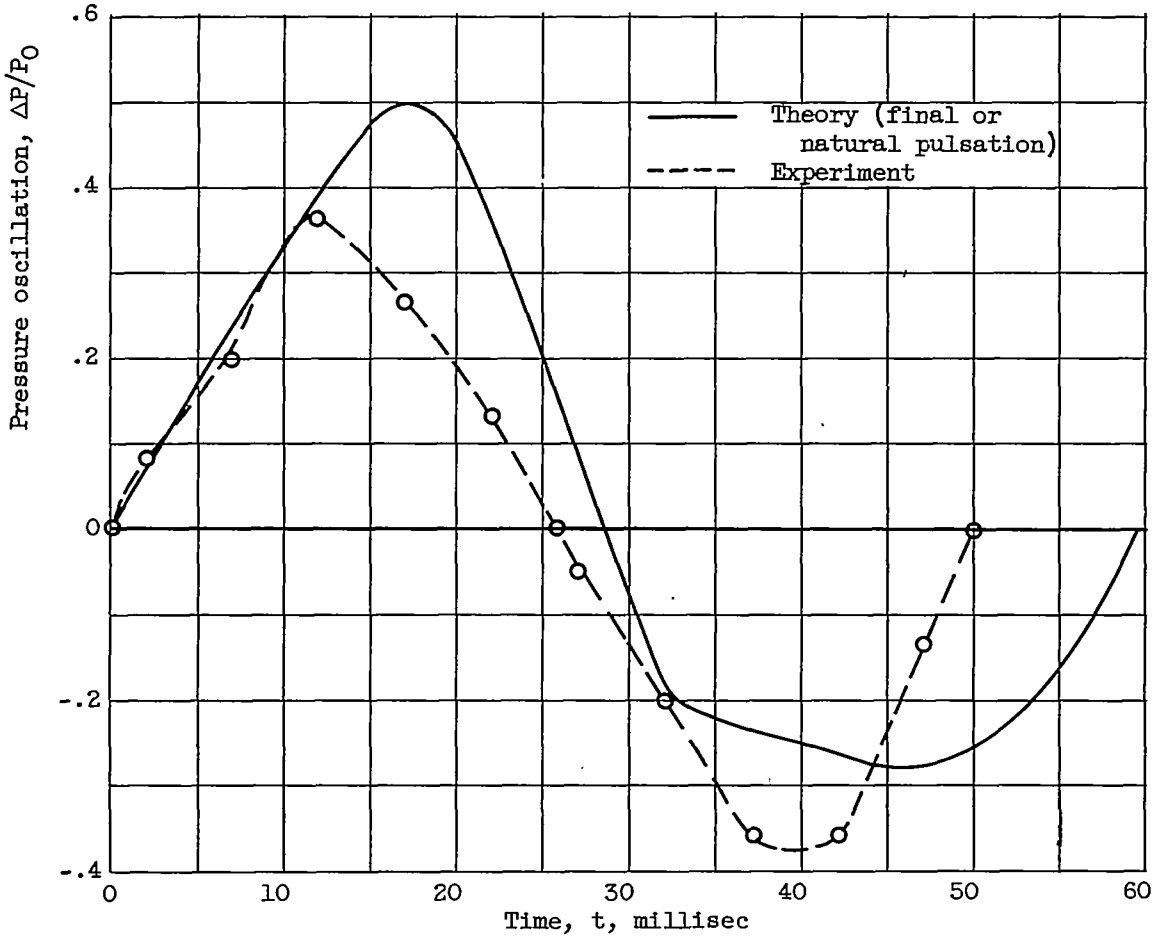

(b) Mass-flow ratio: experiment, 0.41; theory, 0.40.

Figure 6. - Comparison of theoretical pressure-time variation with experiment for high-mass-flow-ratio diffuser (small volume engine).

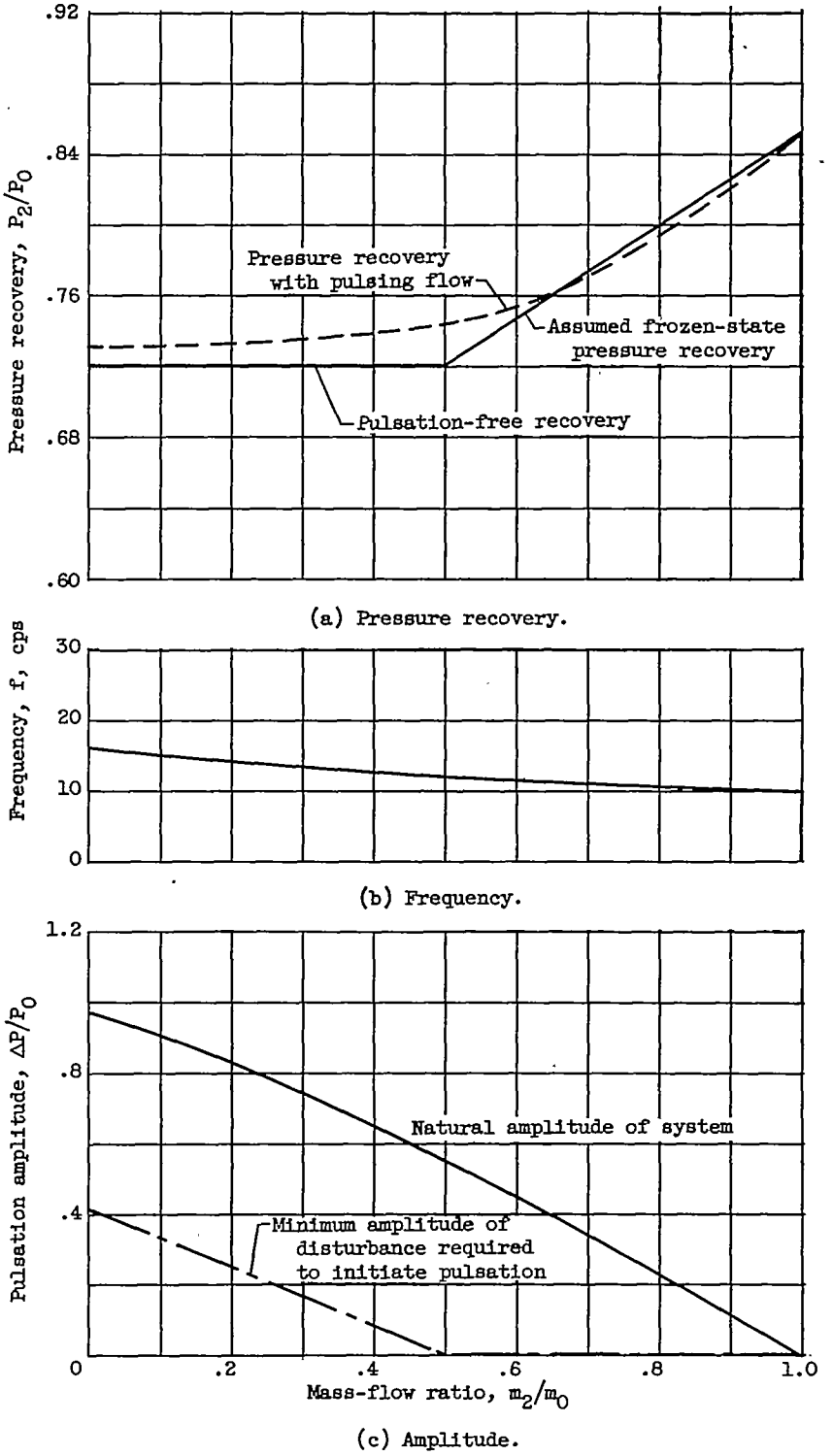

Figure 7. - Stability characteristics and theoretical pulsation amplitude and frequency variation with mass-flow ratio for hypothetical ram-jet engine with arbitrary perforated, convergent-divergent, open-nosed diffuser.

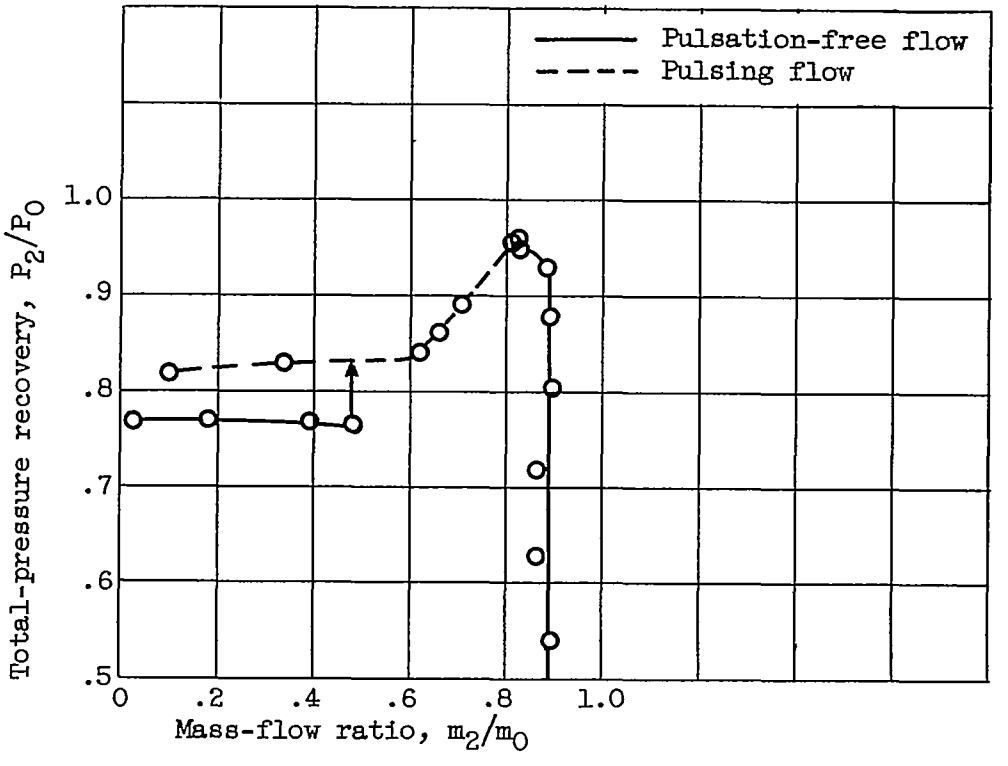

Figure 8. - Pulsation hysteresis and effect of flow pulsation on diffuser pressure recovery. Perforated, convergent-divergent diffuser. Experimental inlet 1.63-e (ref. 7).

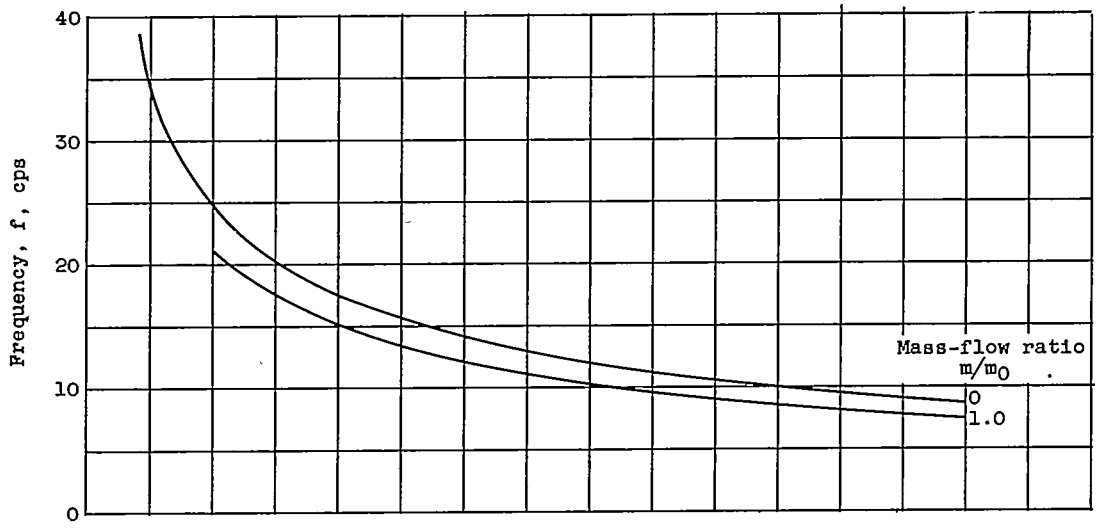

(a) Frequency.

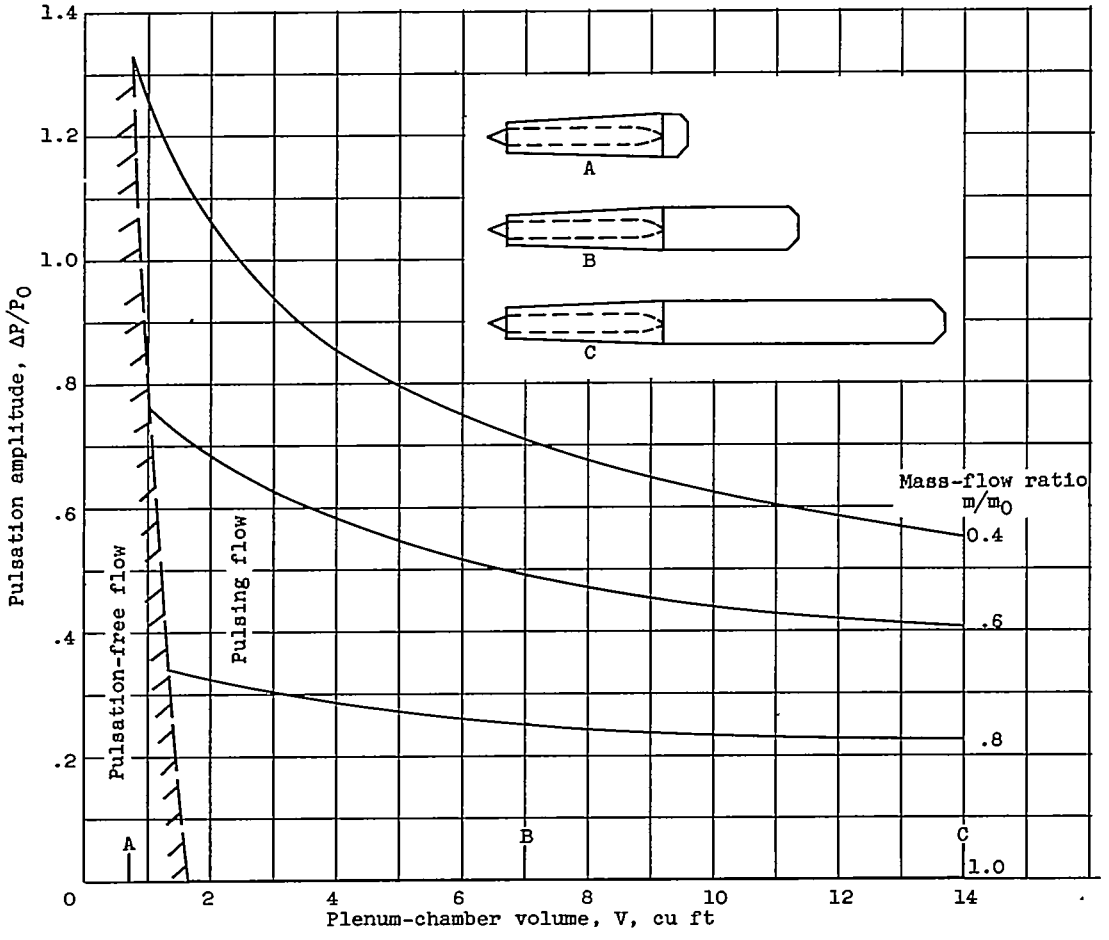

(b) Amplitude.

Figure 9. - Theoretical effect of plenum-chamber volume on diffuser stability, pulsation amplitude and frequency. Arbitrary, hypothetical ram-jet engine with constant air-column volume.

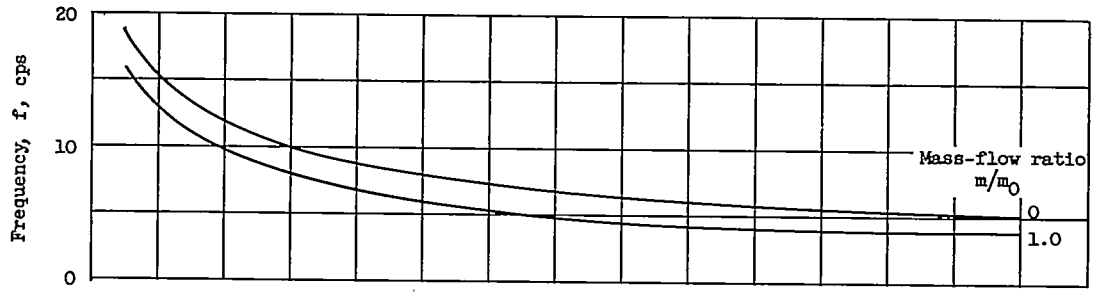

(a) Frequency.

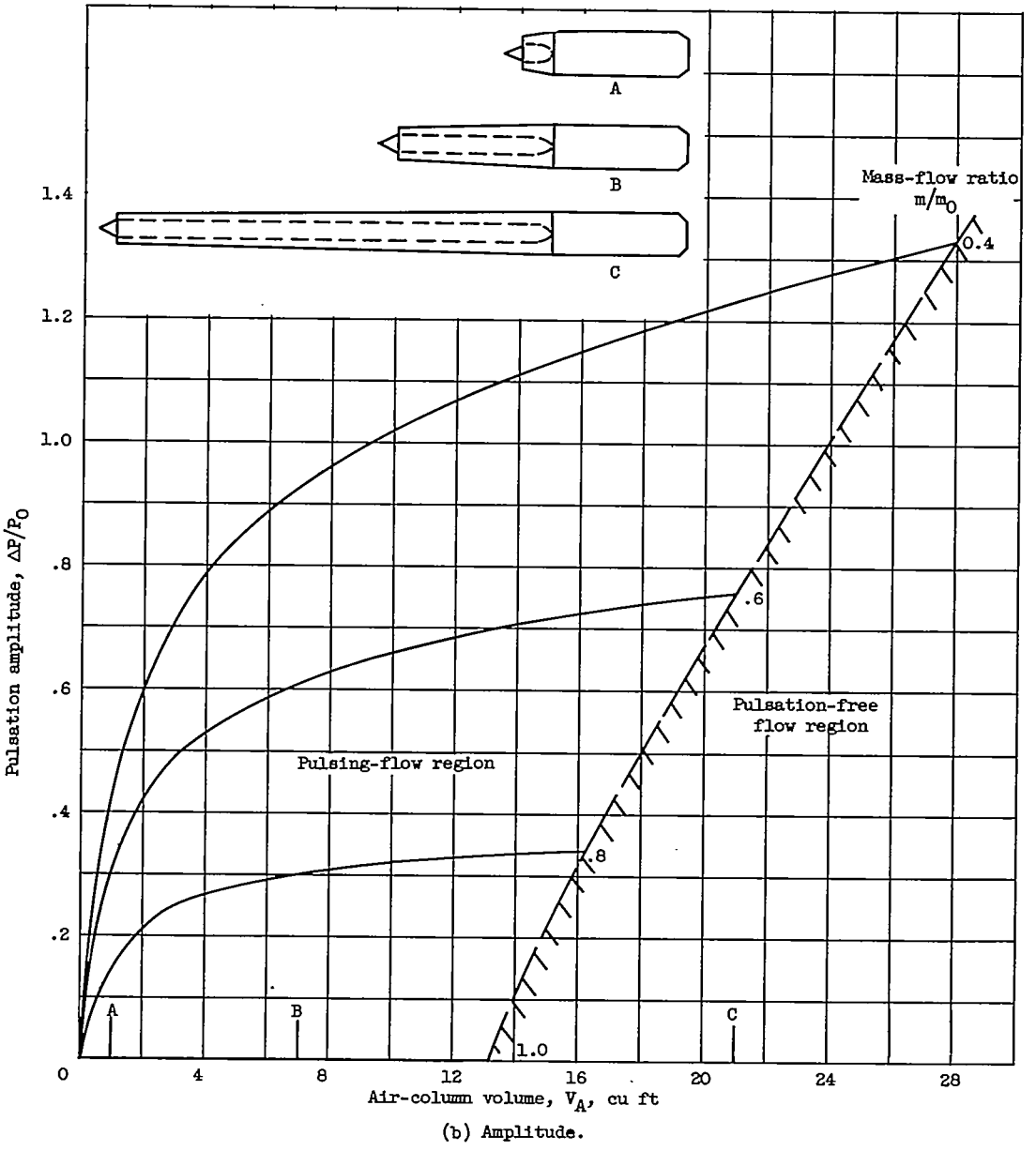

(b) Amplitude.

Figure 10. - Theoretical effect of air-column volume on diffuser stability and pulsation amplitude and frequency. Arbitrary, hypothetical ram-jet engine with constant plenum-chamber volume.